Perylene based PET fluorescent molecular probes for pH monitoring

Ayedah Tariq, Ulysse Garnier, Rasta Ghasemi, Jean Pierre Lefevre, Cédric Mongin, Arnaud Brosseau, Jean Frédéric Audibert, Robert Pansu, Alexandre Dauzères, Isabelle Leray

Journal of Photochemistry & Photobiology, A: Chemistry 432 (2022) 114035

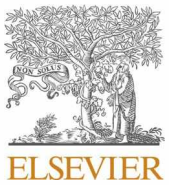

Contents lists available at ScienceDirect

Journal of Photochemistry & Photobiology, A: Chemistry

journal homepage: www.elsevier.com/locate/jphotochem

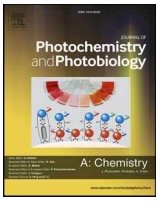

Perylene based PET fluorescent molecular probes for pH monitoring

Ayedah Tariq [a,b], Ulysse Garnier [a], Rasta Ghasemi [c], Jean Pierre Lefevre [a,d], Cédric Mongin [a], Arnaud Brosseau [a], Jean Frédéric Audibert [a], Robert. Pansu [e], Alexandre Dauzères [b], Isabelle Leray [a,*]

[a] Université Paris-Saclay, ENS Paris-Saclay, CNRS, PPSM, 91190 Gif-sur-Yvette, France
[b] Institut de Radioprotection et de Sureté Nucléaire, IRSN/PSE-ENV/SEDRE/LETIS, BP 17, 92262 Fontenay-aux-Roses Cedex, France
[c] Université Paris-Saclay, ENS Paris-Saclay, CNRS, IDA, 91190 Gif-sur-Yvette, France
[d] Conservatoire National des Arts et Métiers, 292 rue Saint-Martin, 75003 Paris, France
[e] Université Paris-Saclay, ENS Paris-Saclay, CNRS, LUMIN, 91190 Gif-sur-Yvette, France

ARTICLE INFO

Keywords:
Fluorescent probe
pH sensor
Optical fiber sensor
Optode
Hydrogel

ABSTRACT

New perylene-based pH probes have been synthesized and utilized for the development of pH optodes. These amine-functionalized perylene-based probes display high molar absorption coefficients in the visible range and protonated forms are characterized by fluorescence quantum yields close to unity. By deprotonation, a strong fluorescence quenching occurs due to an efficient PET-type mechanism. These molecules have been immobilized in two types of polymer (PVA-GA and HydroMed D4). Photophysical studies of these materials revealed heterogeneity in the distribution of the molecules inside the polymer matrix. Finally, optodes have been developed for the measurement of pH between 8 and 10 with promising photostability and sensibility results.

1. Introduction

pH value is one of the key parameters for a wide range of applications such as biomedical studies, environmental water quality control or materials ageing monitoring. In biology, pH measurement is an essential parameter for monitoring bacterial growth [1] or for diagnosis of numerous pathologies such as Alzheimer's [2] or certain cancers [3]. If the use of pH-meters based on proton-selective electrodes has proven to be efficient in many fields, in some cases they are not usable (intense electric field, remote measurements and pH measurement at the micrometer scale). In this context, optical methods and in particular, those based on fluorescence variation, have many advantages in terms of response time, low cost and possibility of use in extreme environments by means of fiber optics [4].

Therefore, several optical sensors have already been reported in the literature for in situ pH measurement [5]. These optical sensors are based on the exploitation of fluorescent probes embedded in polymer matrices. The nature of the fluorescent probes determines the sensitivity and photostability of the final optical sensors. Numerous pH sensors are based on BODIPY [6] or naphthalimide fluorophores [7–9] but with some drawbacks in terms of brightness. In this context, perylene based fluorophores are very attractive because of their high photostability [10]. The large majority of fluorescent pH probes are derived from perylene diimide. Although they have remarkable photophysical properties, these compounds are not stable in alkaline conditions.

In the course of our recent ongoing program directed on the design of pH optodes operating in high pH media, we have decided to focus our attention on perylene based amine fluorophores. Indeed, Pandith et al. recently described the synthesis and photophysical studies of 3-amino substituted perylene. In particular they described the synthesis of a compound bearing an imidazole function for the recognition of salicylic acid derivatives [11]. In this context, we have decided to evaluate the ability of perylene based amines to act as fluorescent probes for pH measurement. In the present work, we herein report the synthesis, the photophysical characterization, and the acido-basic properties of three perylene based alkylamine fluorescent probes. In addition, we describe the development of a pH optode setup and the ability to use these molecules for efficient pH monitoring as well as the impact of the embedding strategy on their physicochemical, sensitivity and photostability properties.

* Corresponding author.
E-mail address: isabelle.leray@ens-paris-saclay.fr (I. Leray).

https://doi.org/10.1016/j.jphotochem.2022.114035
Received 6 January 2022; Received in revised form 1 May 2022; Accepted 18 May 2022
Available online 23 May 2022

2. Experimental section

2.1. Reagents and general techniques

All reagents were purchased from Sigma-Aldrich and were used without further purification. NMR spectra were recorded on a JEOL-FT NMR 400 MHz spectrometer using $CDCl_3$, CD_3OD or DMSO-d_6 as solvent and tetramethylsilane as internal standard. Data are reported as follow: chemical shift in ppm (δ), multiplicity (s = singlet, d = doublet, t = triplet, m = multiplet), number or protons. This work has benefited from the facilities and expertise of the Small Molecule Mass Spectrometry platform of ICSN (Centre de Recherche de Gif – https://www.icsn.cnrs-gif.fr).

2.2. Synthesis of the probes

N-(perylen-3-ylmethyl)octan-1-amine (1): 3-formylperylene [12] (285 mg, 1.02 mmol), 1.7 mL of octylamine (10,2 mmol, 10 equiv.), 5.2 mg of paratoluene sulfonic acid (0.03 mmol, 0.03 equiv.) and 30 mL of toluene was placed in a three-neck round-bottomed flask equipped with a Dean–Stark trap. The reaction mixture was stirred under reflux for 4 h and then cooled, diluted with ethanol (half of the volume of toluene) and cooled to 0 °C with an ice bath. Solid $NaBH_4$ (2 equiv.) was added to the stirred mixture while maintaining the temperature below 15 °C and then the stirring was continued for 12 h at room temperature. After addition of water, the reaction mixture was extracted with dichloromethane. The organic phase was washed with a saturated solution of $NaHCO_3$ and water. The organic phase was dried over $MgSO_4$ and concentrated. The product was isolated by precipitation in MeOH to afford 232 mg of pure compound **1** (58 %).

^{1}H NMR (400 MHz, $CDCl_3$) δ 8.21–8.11 (m, 4H, Pery), 7.93. (d, J = 8.7 Hz, 1H),7.66 (dd, J = 7.8 Hz, J2.8 Hz, 1H), 7.53–7.43 (m, 4H), 4.15 (s, 2H), 2.75 (t, J = 7.33 Hz, 2H), 1.57–1.53(m, 2H), 1.38–1.25(m, 10*H*), 0.88 (t, J = 6.9 Hz, 3H),

13C NMR (100 MHz, $CDCl_3$) δ 135.44, 134.70, 133.05, 131.84, 131.38, 131.29, 130.72, 129.16, 128.56, 127.90, 127.75, 126.97, 126.77, 126.63, 123.46, 120.35, 120.27, 120.13, 119.90, 51.60, 49.96, 31.94, 30.01, 29.62, 29.40, 27.48, 22.77,14.22.

C 29H 31 N.

HRMS: $C_{29}H_{31}N$ − 393.2454 $[M + H]^+$.

HRMS: Calculated for: $C_{29}H_{31}N$ -$[M + H]^+$ 393.2457 found 393.2454.

N-methyl-N-(perylen-3-ylmethyl)octan-1-amine (2): 170 mg (0.43 mmol) of **1** was dissolved in 20 mL of 1,2 dichloroethane. 915 mg of $NaBH(OAc)_3$ (4.32 mmol, 10 equiv.) was added to the mixture and 0.5 mL of formaldehyde solution (37% wt in H_2O) was added slowly over a period of 30 min. After 14 h of reaction, the solution was diluted with 25 mL of dichloromethane and the organic solution was washed with a saturated solution of $NaHCO_3$ and water. The organic phase was dried over $MgSO_4$ and concentrated to give 140 mg of pure compound (60 %).

1H NMR (400 MHz, $CDCl_3$) δ 8.23–8.14 (m, 5H, Pery), 7.70 (d, J = 7.8 Hz, 2H), 7.56–7.45 (m, 4H), 3.84 (s, 2H), 2.50 (t, J = 7.33 Hz, 2H), 2.26 (s, 3H), 1.62–1.30(m, 2H), 1.38–1.25(m, 10*H*), 0.88 (t, J = 6.9 Hz, 3H),

13C NMR (100 MHz, $CDCl_3$) δ 134.67 133.75, 131.51, 131.41, 130.67, 129.12, 128.51, 128.2, 128.0, 127.65, 127.58, 127.01, 126.61, 126.34, 124.7,2 120.19, 120.15, 119.93, 119.60, 119.10, 61.07, 58.15, 42.36, 31.90, 29.54, 27.54, 24.93,22.70, 14.111.

HRMS: Calculated for $C_{30}H_{33}N$ -$[M + H]^+$ 407.26080 found 407.262275.

2,2′-((perylen-3-ylmethyl)azanediyl)bis(ethan-1-ol) (3): 3-formylperylene (400 mg, 1.42 mmole), 1.35 mL of diethanolamine (14.2 mmol, 10 equiv.), 7.4 mg of paratoluene sulfonic acid (0.042 mmol, 0.03 equiv.) and 45 mL of toluene was placed in a three-neck round-bottomed flask equipped with a Dean–Stark trap. The reaction mixture was stirred under reflux for 4 h and then cooled. 20 mL of ethanol was added to the mixture and 142 mg of NaBH4 (2 equiv.) was added to the stirred mixture while maintaining the temperature below 15 °C and then the stirring was continued for 12 h at room temperature. After addition of water, the reaction mixture was extracted with dichloromethane. The organic phase was washed with water, dried over $MgSO_4$ and concentrated. The product was isolated by silica gel column chromatography with CH_2Cl_2 / MeOH/NEt_3 (90/9/1) to afford 210 mg of pure compound **3** (40 %).

1H NMR (400 MHz, $CDCl_3$) δ 8.27–8.02 (m, 5H, Pery), 7.7 (d, J = 7.8 Hz, 2H), 7.57–7.42 (m, 4H), 4.11 (s, 2H), 3.62 (t, J = 5.2 Hz, 4H), 2.83 ((t, J = 5.2 Hz, 4H).

13C NMR (100 MHz, $CDCl_3$) δ 134.70, 134.13, 133.54, 131.91, 131.40, 131.33, 131.16, 129.30, 128.61,128.54, 127.98, 126.91,126.71, 126.66, 123.76,120.49, 120.27, 119.69, 60.09, 59.00, 56.38.

HRMS: Calculated for $C_{25}H_{23}NO_2$ − 369.1729 $[M + H]^+$ found 369.1729.

2.3. Polymers

PVA-GA matrix. PVA (85,000 – 124,000 g/mol) was dissolved in dimethyl sulfoxide – DMSO – at 75 °C, by continuously stirring with an overhead stirrer (Heidolph Overhead Stirrers) during one hour in order to obtain a homogeneous solution with a PVA weight ratio of 10%. The corresponding fluorescent probe was added and stirred in the PVA solution at room temperature, to a weight ratio of 0.45 mg for every 10.0 g of solution. 0.4 mL of an aqueous GA solution (50% by mass in water) was added to obtain a PVA-GA doped solution. The viscous solution was spread on a high density polyethylene HDPE sheet with a 200 µm wire bar applicator and a TQC automatic film applicator (TQC Sheen). The obtained sheet was placed in a desiccator alongside 50 mL of 6 M HCl solution in order to catalyze the reticulation and form chemically cross-linked hydrogels. After 48 h of reticulation under reduced pressure, the PVA-GA cross-linked hydrogel was washed three times with deionized water to remove any acid and DMSO traces. Doped hydrogels were dried at room temperature and rehydrated for one hour prior their utilization. The thickness of dehydrated PVA-GA films was measured with a digital micrometer (Mitutoyo MDC-25MX) and averaged on ten samples. The average thickness of hydrated films was 86 ± 5 µm.

Hydromed D4 matrix. HydroMed™ D4 (AdvanSource Biomaterials) was dissolved in tetrahydrofuran THF by stirring with a magnetic stirrer during one hour at room temperature in order to obtain a homogeneous solution with a HydroMed™ D4 ratio of 10%. The corresponding fluorescent probe was stirred in to a weight ratio of 0.5 mg for every 11.0 g of solution. The mixture was drop casted in a custom-made polytetrafluoroethylene – PTFE – mold. The solvent was removed in a two-step process: first a slow evaporation step was conducted by placing the mold on a hot plate at 50 °C, followed by a complete evaporation in a desiccator under vacuum for two hours. The thickness of hydrated HydroMed™ D4 films was measured with a digital micrometer (Mitutoyo MDC-25MX) and averaged on ten samples. The average thickness of HydroMed™ D4 films was 161 ± 5 µm.

Emission and absorbance spectra were recorded in quartz cuvettes at room temperature on a FluoroMax series 4 spectrofluorometer (HORIBA Scientific) and on a Cary series 5000 UV–Vis-NIR spectrophotometer (Agilent Technologies), respectively. Solid-state fluorescence quantum yields were measured using an integrating sphere (F-3018 from Horiba Jobin-Yvon, internal diameter 102 mm) mounted on a Fluorolog 3 from HORIBA Scientific.

Fluorescence of the samples is recorded using an inverted microscope for epifluorescence (TE2000-U, Nikon) (figure SI1). The samples are positioned at the objective focal plane (CFI Plan Fluor 40X, N.A. 0.75) and excited at 343 nm in a widefield mode using the THG of the native pulsed output of a femtosecond Yb:KGW laser (t-pulse 200, Amplitude Systemes, repetition rate 10 MHz, pulse width 400 fs).The

emitted photons are collected with a time and space-resolved single photon camera - LINCam [13] Fluorescence decays of the sample are extracted from the entire field of view of the detector ca. Ø60 µm. QA–Fluorescence Life time Imaging (FLIM) - LINCamIs a time and space single photon counting camera Quadrant Anode MCP-PM based photo-detector operating in TCSPC mode. Each photon is digitalized in a 12 bits array in position and Time–Tagged–Time–Resolved (TTTR) with a time resolution of 10 ns and 50 ps respectively. Hardware, electronic interface and GUI are maintained by Photonscore, Germany; coupling optical setup, calibration, post processing and analysis tools software are managed in our team (Dr R. PANSU (LUMIN), J.-F. AUDIBERT (PPSM)).

2.4. Optode set up

An optode setup was developed in order to measure efficiently the pH of solutions (Fig. 1). Doped polymer matrices were cut and placed in a custom-made sample compartment consisting of a hollowed cylinder made out of black polyoxomethylene (DELRIN®) and mounted with a glass slide. An SMA connector has been added to ensure the connection of an optical fiber. Cut pellets of the selected doped matrix are directly installed on the glass slide and a hollowed cap maintains the sample in place while allowing a direct contact with the studied environment. A light emitting diode LED (Roithner LED405-30 M32), selected for its spectral band of radiation peaking at 405 nm, illuminates the sample through optical fibers. A pulsed signal was used in order to limit the pH probes photobleaching (pulse width: 650 µs, T = 13 ms, A = 4 Vpp, edge time: 5 ns) and a lock-in amplifier (7265 Dual Phase DSP Lock-In Amplifier Ametek Scientific Instruments) was connected to extract the signal. A dichroic mirror (414 nm edge Semrock FF414-Di01) was installed to split the excitation and the emission beam and then the latter is directed to a photomultiplier tube PMT (Hamamatsu 722–10) to ensure signal collection.

Complete emission spectrum of each doped matrix was acquired on a spectrofluorometer (FluoroMax-4, Horiba) fitted with a custom-made optical arrangement similar to the optode setup (Fig. 2). The optical arrangement consisted of a light emitting diode LED (Roithner LED405-30 M32, $\lambda_{emission,\ max}$ = 405 nm) mounted with a focalizing lens and a band pass filter centered at 405 nm, with a 10 nm bandwidth. An optical fiber connects the LED to a three-way optical cube equipped with a dichroic mirror (414 nm edge Semrock FF414-Di01) in order to split the excitation and emission beam. The sample compartment described previously is fitted with an optical fiber allowing excitation and signal collection through the dichroic mirror, the third optical fiber being connected to the spectrofluorometer to acquire the emission spectrum of the sample.

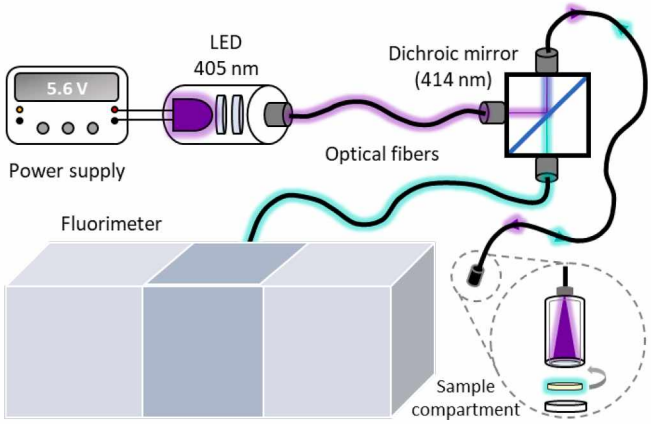

Fig. 2. Diagram of the optical setup developed to study the emission of hydrogels doped with perylene based pH probes.

3. Results and discussion

3.1. Synthesis of the probes

The synthesis of the perylene based pH molecular sensors is presented on Scheme 1. Compounds **1** and **3** are synthesized by reaction of 3-formylperylene [12] with octylamine and diethanolamine (10 equiv.) in the presence of paratoluene sulfonic acid (0.03 equiv.) in toluene, followed by $NaBH_4$ (10 equiv.) treatment [14]. Compounds **1** and **3** were obtained in 58 and 40% yield, respectively. Methylation of compound **1** was performed by reductive amination with formaldehyde [15] to obtain compound **3** in 60% yield. Compounds **1**, **2** and **3** have been characterized by ^{1}H / ^{13}C NMR and HRMS analysis.

3.2. Photophysical properties

The photophysical properties of the perylene derivatives were studied in a DMSO/water mixture. Due to the high hydrophobicity of the perylene core, the maximum proportion of water was limited to 20% v:v to ensure complete solubility and satisfactory results. The photophysical characteristics are given in Table 1. The absorption of the perylene derivative displayed three well-defined intense absorption bands attributed to S1 ← S0 (ππ*) transition. For example in the compound **3**, (Fig. 3)

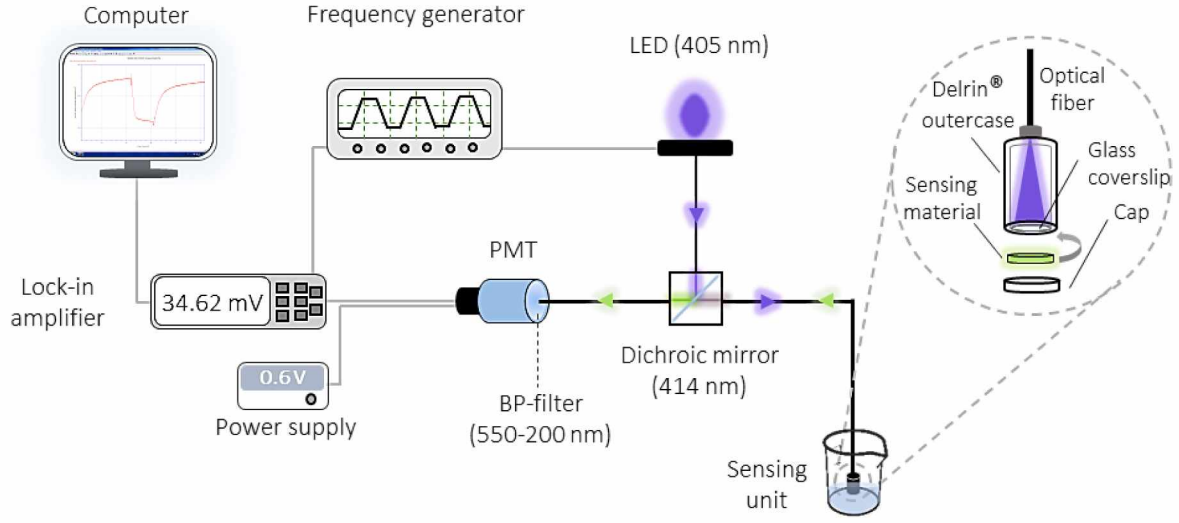

Fig. 1. pH optode setup based on the perylene based fluorescent probes.

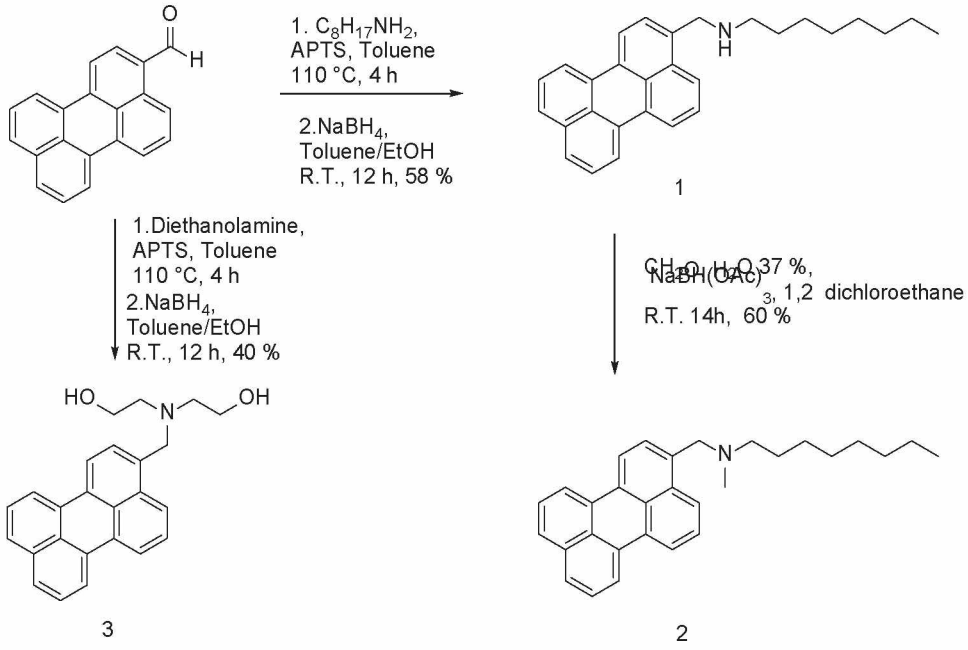

Scheme 1. Synthesis scheme of perylene based pH probes.

Table 1
Photophysical properties of perylene dyes in DMSO/water mixture (8:2 v/v). Absorption maxima (λ_{abs}), molar absorption coefficients (ε), emission maxima (λ_{em}), fluorescence quantum yields (ΦF), and fluorescence lifetimes (τ) for the acidic and basic forms. The basic form was generated by addition of [OH^-] at 10^{-3} mol.L^{-1}.

Compound	λ_{abs}(nm)	ε ($M^{-1}.cm^{-1}$)	λ_{em} (nm)	$\Phi_F(NH^+)$	$\Phi_F N$	τ(NH^+) (ns)	τ(N) (ns)
1	394, 419, 445		451, 480, 514	0.88	0.17	–	–
2	396, 419, 446	34 800	454, 484, 516	0.71	0.02	4.77	0.2
3	397, 420, 446	36 650	455, 486, 517	0.82	0.07	4.76	0.14

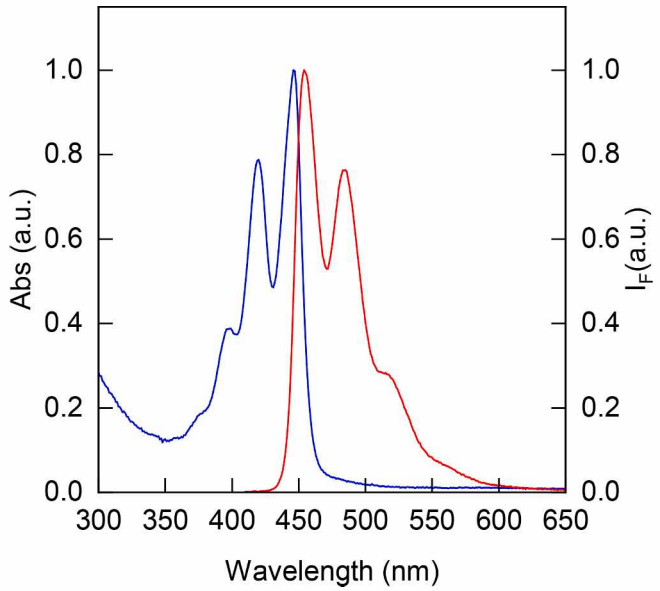

Fig. 3. Normalized absorption (blue line) and emission (red line) spectra of **3** DMSO/water mixture (8:2 v/v); λ_{exc} = 405 nm; **[3]** = 5.8 μM).

the absorption bands are located at 446, 420 and 397 nm, respectively. The emission spectra of the compound in the acid form is the perfect mirror image of the absorption band with a small Stokes shift (10 nm) attributed to the LE emission state. The brightness of the dyes in the acid form (defined as the product of the molar absorption coefficients and fluorescence quantum yields – Brightness = $\varepsilon(\lambda_{exc}) \times \Phi_F$) is excellent: 24,700 and 30,050 for 2 and 3, respectively. Time-resolved fluorescence measurements were performed by single-photon counting with pico-second Ti:Sa laser excitation at 405 nm**.** The fluorescence lifetimes of the acid forms which have been determined by non linear-curve fitting by considering biexponential time decay,are in a range of 4.8 ns to 5.2 ns (Table 1), which is typical for perylene fluorophores [16]. A strong quenching of the emission is observed upon deprotonation of the dye because of an efficient PET process occurring from the alkylamino group to the perylene core. In the case of **2** and **3**, the quenching efficiency is

Table 2
pH sensing properties of perylene dyes in solution (DMSO/water mixture (8:2 v/v)) and embedded in polymer films PVA-GA or Hydromed D4 (pKa and fluorescence quenching (Imax/I_0), response time t_{90} of the obtained sensor.

Compound	DMSO/water (8:2 v/v)		PVA-GA			HydroMed D4		
	pKa	$\frac{I_{max}}{I_0}$	pKa	$\frac{I_{max}}{I_0}$	t_{90} (s)	pKa	$\frac{I_{max}}{I_0}$ Imax/I0	t_{90} (s)
1	9.78 ± 0.02	0.33	–	–	–			
2	11.31 ± 0.02	0.06	7.36	0.63	148	6.39	0.88	335
3	11.36 ± 0.02	0.09	7.02	0.67	163	5.84	0.79	257

equal to 10 and it is lower for **1** due to the presence of the secondary amine since the energy difference is lower.Table 2.

Such effect can be easily explained by considering the Rehm-Weller equation (2).

$$\Delta G^0 = F\left[E^0(D^+/D) - E^0(A/A^-) - \Delta E_{00}(A)\right] \quad (2)$$

where F is the Faraday constant.

$E^0(D^+/D)$ *is the oxydation potential of the amine moiety*

$E^0(A/A^-)$ *is the reduction potential of the perylene moiety*

- $\Delta E_{00}(A)$: Energy of the perylene moiety expressed in eV

By considering the oxydation potential of the amine moiety of 0.96 V and the reduction potential of perylene of _-1.67 V [17], 2.76 ev $\Delta E_{00}(A)$, it is noticed that this reaction is highly exergonic. In contrast, with the secondary amine with an oxidation potential of 1.3 V the Gibbs free energy change (ΔG) is lower.

The lifetime of the neutral form is significantly shorter and a decay time of 140 ps has been found in the case of the compound **3**. The radiative and nonradiative rate constants are related to the corresponding emission quantum yield and lifetime by $k_r = \Phi_F/\tau_F$ and $k_{nr} = (1\text{-}\Phi_F)/\tau_F$. As expected, for the neutral form of the perylene dyes, an increase of the non-radiative decay rate knr is observed by comparison of the acid form (6.6 10^9 s^{-1} for N and 3.7 10^6 s^{-1} for NH^+).

3.3. pH sensing properties in solution

The pH sensitivity of perylene dyes **1**, **2** and **3** were investigated in a DMSO/water mixture (8:2 v/v). As expected under basic condition, the formation of the amino group induces a strong inhibition of the emission (Fig. 4). Referring to the Henderson–Hasselbalch equation, it is possible to link the pH to the ratio of protonated/deprotonated probe concentrations (Eq. (1)). Thus, three parameters were defined: IF_{Max} is the maximum intensity of fluorescence observed when the probe is fully deprotonated, and IF_{Min} will be linked to the fully protonated state. As the probe is distributed in a solid matrix and not dissolved in solution, an additional factor dpH is introduced to take the distribution of pKa into account [18]. Thus, plotting the intensity at 525 nm against the calculated pH and fitting the data with Eq. (1) using the software Origin Lab 2018, with a Levenberg Marquardt iteration and a least square method led to a pKa of 9.78.

$$I_F = \frac{I_{FMin} + I_{FMax} \times 10^{\left(\frac{pH\ pKa}{dpH}\right)}}{10^{\left(\frac{pH\ pKa}{dpH}\right)} + 1} \quad (1)$$

For the probe **1**, we noticed that the fluorescence decrease upon deprotonation is about 75%. However, for molecules **2** and **3** variations occur over a narrow pH range. Aggregation of the perylene probes may be at the origin of this effect as already shown by Lee et al. [19–20]. A process of energy transfer in these aggregates can induce the observed amplified inhibition of fluorescence.

3.4. Investigation of the photophysical properties of doped polymer films

In order to perform in situ pH measurements, perylene derivatives **2** and **3** were immobilized in polymer matrices. Hydrophilic polymers were chosen to ensure efficient diffusion of the hydroxyl ions and two polymers were selected: (i) PVA-GA which we had previously reported for a naphthalimide-based optode [5] and (ii) HydroMed D4, a commercially available polyurethane hydrogel consisting of hydrophilic and hydrophobic domains which is widely documented in the literature for pH optodes [6]. The concentration of the dye for each polymer was set at 1 μmol.g^{-1}.

As shown in Fig. 5 for compounds **2** and **3**, a broadening and red-shifting of the emission spectra is observed in the polymer matrix. This effect can be explained by the formation of dye aggregates in the polymer. It should be noted that this effect is more pronounced for the D4 polymer than for PVA-GA, which can be explained by a better solubilization of the perylene dyes in PVA-GA polymeric chains. Time-resolved fluorescence measurements have been performed to get more information on the organization of the fluorophores in the polymer (Fig. 6). As expected, time-resolved fluorescence profiles show multi-exponential decays. Satisfactory fits can be obtained by considering 3 exponentials with corresponding decay times of 0.4 ns, 3.5 ns and 6 ns for **2** and **3** in HydroMed D4 (table 2SI). The short decay times are in good agreement with those obtained in solution for the acid and neutral perylene dyes and the longest component could be attributed to the formation of perylene aggregates. [21].

The fluorescence changes upon deprotonation of polymer films containing dyes have been studied for dye **2** and **3** in PVA-GA and HydroMed D4. An example of the evolution of the emission spectra is displayed in Fig. 7 for **3** in PVA-GA and Fig. 8 for **2** in Hydromed D4. The pKa values and the quenching efficiencies are given in Table 2. As

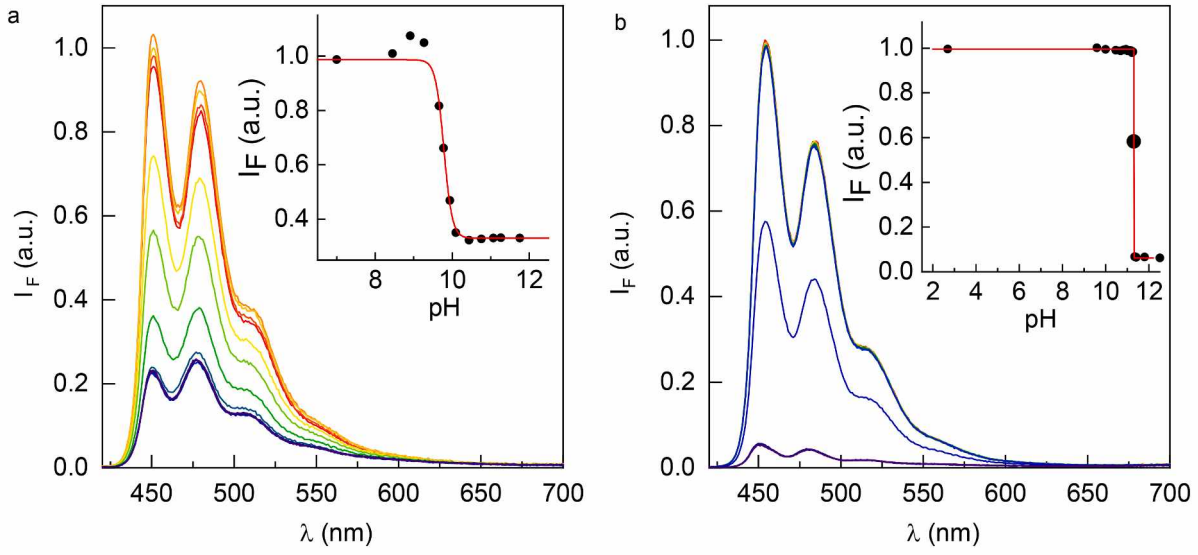

Fig. 4. Effect of NaOH addition on the emission spectra of **1(a))** [5.8 μM] and **3**(b) [1.7 μM] in DMSO/water 8:2 (v/v), λ_{exc} = 405 nm; Inset: Evolution of the fluorescence intensity upon pseudo pH variation, and fitting using eq. (1).

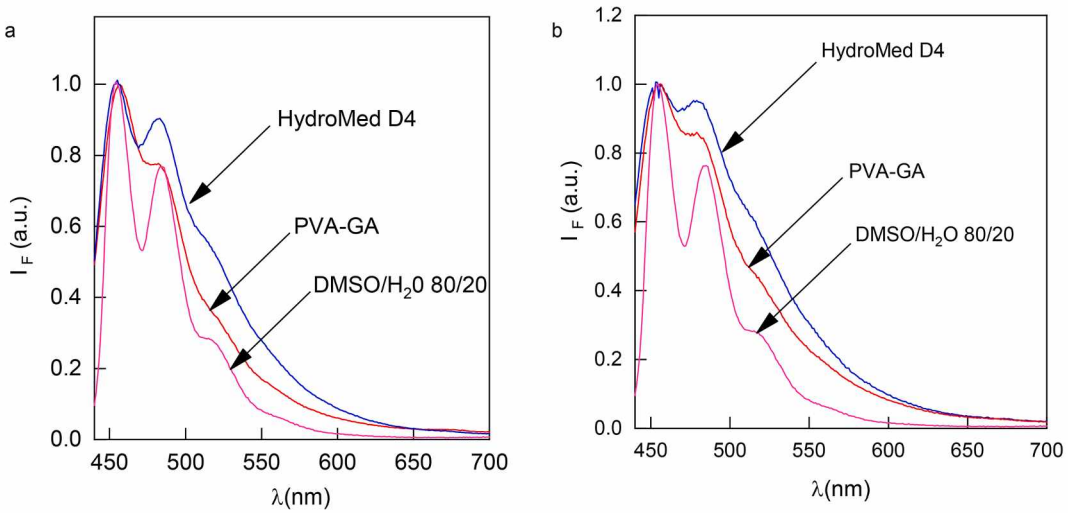

Fig. 5. Emission spectra of compound **2(a) and 3 (b)** in DMSO/water mixture (8:2 v/v) and immobilized in HydroMed D4 and PVA-GA polymers. (λ_{exc} = 405 nm).

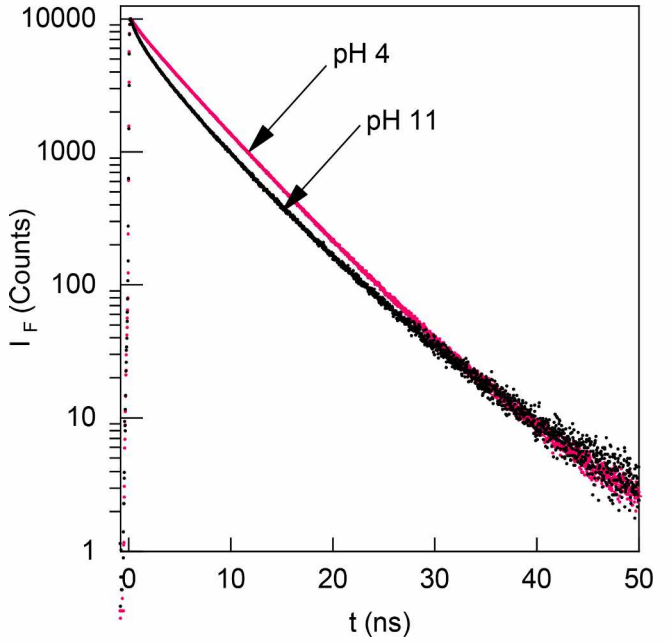

Fig. 6. Fluorescence decays (λ_{exc} = 405 nm) of **3** in PVA-GA at pH 4 and pH 11 (λ_{em} = 470 nm).

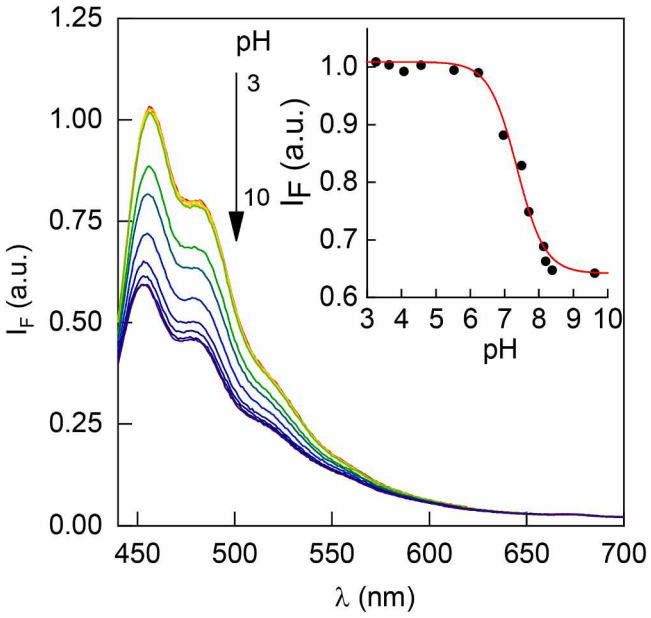

Fig. 7. Emission spectra of **3** in PVA-GA upon pH titration; inset: evolution of the integrated fluorescence upon pH variation.

previously reported for PET based amino fluorescence probes [22], a significant decrease of the apparent pKa is observed because of strong interaction between the matrix and the dyes. It should also be noted that the efficiency of fluorescence quenching is not 100% and at most it reaches 40% in the case of **3** in PVA-GA. This may be due to a partial accessibility of the fluorophores for the hydroxide anions in the polymer matrix due to a dispersion of the dyes in hydrophobic domains. This effect is more pronounced in the case of HydroMed D4, where polymer chains are composed of co-polymerized hydrophobic and hydrophilic blocks, compared to PVA-GA [23].

Thus, we envisioned performing FLIM experiments to unveil the presence microdomains but unfortunately, the spatial resolution of the experimental setup does not allow to get clear images of these potential domains. Regarding the decays, as observed in stationary fluorescence experiments, a quenching of the average time decay was observed.

3.5. *Photostability and reversibility*

The reversibility and time response of the films is a key parameter for the design of an optode. For PVA-GA and HydroMed D4 films with an average thickness of 86 ± 5 µm and 161 ± 5 µm respectively, short average response times of t_{90} = 155 s and t_{90} = 405 s respectively were obtained when shifting from pH = 4 to pH = 9 (Fig. 9). Repeating this cycle for several times on polymer samples gave comparable results thus indicating the reversibility and reproducibility of the signals. As expected for the polymer containing perylene, thin films have shown a very good photostability for prolonged LED exposure in acid and basic pH (Fig. 9).

4. Conclusion

In this work, novel perylene-based chromophores bearing amine functions were synthesized and chosen for their suitable excitation/emission wavelength ranges and remarkable photostability as alkaline

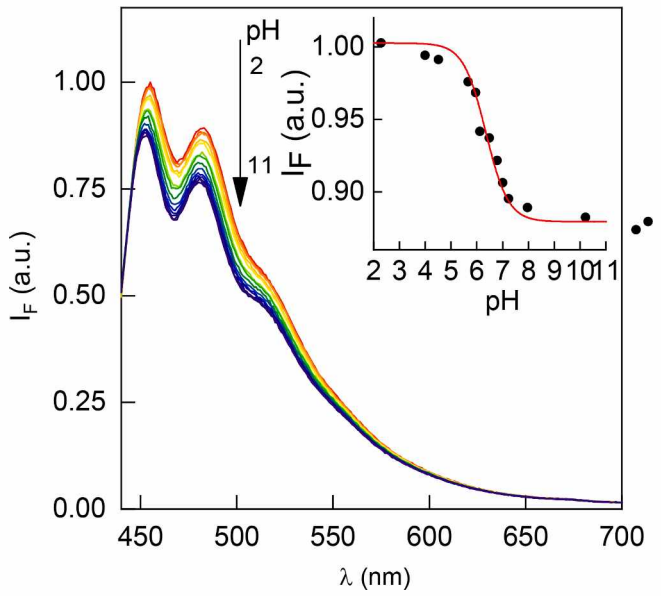

Fig. 8. Emission spectra of **2** in HydroMed D4 upon pH titration; inset: evolution of the integrated fluorescence upon pH variation.

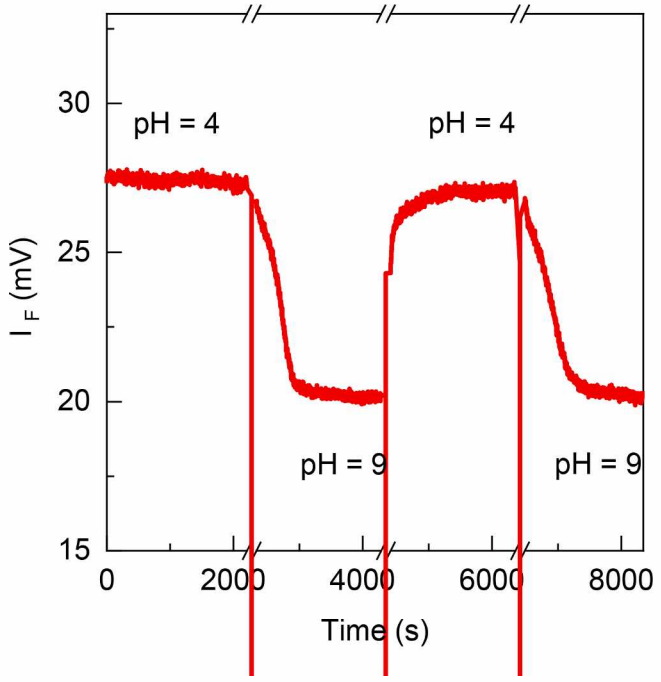

Fig. 9. Fluorescence intensity of compound **3** entrapped in PVA-GA as function of pH, at room temperature, $\lambda_{exc} = 405$ nm. Data acquired on the optode setup, adjacent averaging (10 pts). A change of optical index upon change of buffer solution has been overlooked by introducing breaks in the x-axis.

pH probes. The probes were immobilized in two types of polymer PVA-GA and HydroMed D4 and their pH sensing abilities were demonstrated in solution. Extensive photophysical studies were carried out to prove the heterogeneity in probes distribution in the polymers. A small proportion of excimer was found and changes in the photophysical properties were found to be dependent on pH. We were able to show that a large proportion of trapped probes were not accessible to pH changes. Specific interactions between the probes and the matrices lead to a consequent shift in the pH range that can be studied with the developed optodes. An efficient pH optode setup was developed and doped polymers showed very good photostability upon continuous irradiation, with short response time ranging from 150 s for the compound **2** entrapped in a PVA-GA matrix, to 335 s for the same compound entrapped in a thicker HydroMed D4 matrix.

CRediT authorship contribution statement

Ayedah Tariq: Investigation. **Ulysse Garnier:** Investigation. **Rasta Ghasemi:** Investigation. **Jean Pierre Lefevre:** Conceptualization, Investigation. **Cédric Mongin:** Supervision, Methodology, Conceptualization. **Arnaud Brosseau:** Investigation. **Jean Frédéric Audibert:** Investigation. **Robert. Pansu:** Investigation. **Alexandre Dauzères:** Supervision, Methodology. **Isabelle Leray:** Writing – review & editing, Methodology, Conceptualization.

Declaration of Competing Interest

The authors declare that they have no known competing financial interests or personal relationships that could have appeared to influence the work reported in this paper.

Acknowledgments

The authors gratefully acknowledge financial support by the IRSN.

Appendix A. Supplementary data

Supplementary data to this article can be found online at https://doi.org/10.1016/j.jphotochem.2022.114035.

References

[1] Y. Si, C. Grazon, G. Clavier, J. Rieger, J.F. Audibert, B. Sclavi, R. Meallet-Renault, Biosens. Bioelectron. 75 (2016) 320–327.
[2] A.A. Golabek, E. Kida, M. Walus, W. Kaczmarski, M. Michalewski, K.E. Wisniewski, Mol. Genet. Metab. 70 (2000) 203–213.
[3] B.A. Webb, M. Chimenti, M.P. Jacobson, D.L. Barber, Nat. Rev. Cancer 11 (2011) 671–677.
[4] D. Wencel, T. Abel, C. McDonagh, Anal. Chem. 86 (2014) 15–29.
[5] A. Steinegger, O.S. Wolfbeis, S.M. Borisov, Chem. Rev. 120 (2020) 12357–12489.
[6] R. Gotor, P. Ashokkumar, M. Hecht, K. Keil, K. Rurack, Anal. Chem. 89 (2017) 8437–8444.
[7] A. Tariq, J. Baydoun, C. Remy, R. Ghasemi, J.P. Lefevre, C. Mongin, A. Dauzeres, I. Leray, Sens. Actuators, B (2021) 327.
[8] Y. Wen, W. Zhang, T. Liu, F. Huo, C. Yin, Anal. Chem. 89 (2017) (1874) 11869–11871.
[9] T. Zhang, F. Huo, W. Zhang, J. Chao, C. Yin, Sens. Actuators, B (2021) 345.
[10] L.M. Daffy, A.P. de Silva, H.Q.N. Gunaratne, C. Huber, P.L.M. Lynch, T. Werner, O. S. Wolfbeis, Chem. Eur. J. 4 (1998) 1810–1815.
[11] A. Pandith, G. Hazra, H.S. Kim, Spectrochim. Acta, Part A 178 (2017) 151–159.
[12] K. Kodama, A. Kobayashi, T. Hirose, Tetrahedron Lett. 54 (2013) 5514–5517.
[13] Y. Prokazov, E. Turbin, A. Weber, R. Hartig, W. Zuschratter, J. Instrum. 9 (2014) (2015). C12015-C12015.
[14] U. Asseline, E. Cheng, Tetrahedron Lett. 42 (2001) 9005–9010.
[15] K.S. Gudmundsson, P.R. Sebahar, L.D. Richardson, J.F. Miller, E.M. Turner, J. G. Catalano, A. Spaltenstein, W. Lawrence, M. Thomson, S. Jenkinson, Bioorg. Med. Chem. Lett. 19 (2009) 5048–5052.
[16] R. Harmer, H. Fan, K. Lloyd, S. Doble, J. Avenoso, H. Yan, L.G.C. Rego, L. Gundlach, E. Galoppini, J. Phys. Chem. A 124 (2020) 6330–6343.
[17] M. Montalti, A. Credi, L. Prodi, M.T. Gandolfi, Handbook of Photochemistry, CRC Press, 2006.
[18] T.H. Nguyen, T. Venugopala, S.Y. Chen, T. Sun, K.T.V. Grattan, S.E. Taylor, P.A. M. Basheer, A.E. Long, Sens. Actuators, B 191 (2014) 498–507.
[19] J. Cho, C. Keum, S.G. Lee, S.Y. Lee, Analyst 145 (2020) 7312–7319.
[20] B. Muthuraj, S.R. Chowdhury, S. Mukherjee, G.R. Patra, P.K. Iyer, RSC Adv. 5 (2015) 28211–28218.
[21] H. Tachikawa, L.R. Faulkner, Chem. Phys. Lett. 39 (1976) 436–441.
[22] S. Draxler, M.E. Lippitsch, Sens. Actuators, B 29 (1995) 199–203.
[23] G. Greiner, I. Maier, J. Chem. Soc., Perkin Trans. 2 (2002) 1005–1011.